THEORETICAL AND MATERIAL STUDIES ON THIN-FILM ELECTROLUMINESCENT DEVICES

Sixth Six-Monthly Report for the Period
1 November 1987 - 30 April 1988

Project No. A-4168

Prepared for:

Dr. J. B. Robertson/494
NASA
Langley Research Center
Hampton, VA 23665

Prepared by:

Dr. C. J. Summers, Mr. J. A. Goldman and Dr. K. Brennan
Georgia Tech Research Institute and Microelectronics
Research Center

Georgia Institute of Technology
Atlanta, GA 30332

November 1988

SUMMARY

During this report period work was performed on the modeling of High Field Electronic Transport in Bulk ZnS and ZnSe, and also on the surface cleaning of Si for MBE growth. Some MBE growth runs have also been performed in the Varian GEN II System. A brief outline of the experimental work is given below. A complete write up of this investigation will be given at the end of the next report period when we expect to have completed this investigation. The theoretical studies have been written up as a paper, which is enclosed.

Surface Preparation of Si and MBE Growth of ZnS

Surface Cleaning

The substrates were prepared by both an RCA-type cleaning procedure and an ultra-violet ozone cleaning (UVOC) method. The UVOC procedure seemed to produce similar results as the RCA method, but only required 20 minutes per wafer vs. over 2 hours/wafer required for the RCA method. Optimum oxide desorption temperature was found to be about 850°C. Higher temperatures generally resulted in surface roughening. Attempts are being made to substantially reduce the oxide desorption temperature, thereby reducing the number of native defects at the surface. This approach will use H_2S gas stream to volatilize the oxide.

MBE Growth

Films of ZnS were grown by MBE on Si(100) substrates. Films were grown at ZnS flux levels of 8 - 11×10^{-7} Torr. Substrate temperatures (T_{sub}) ranged from just above room temperature (57°C) to 300°C. Temperature pulsing was found to be deleterious to surface smoothness. Films grown were roughly 0.3 to 1.0 μm thick, and grew at a rate of roughly 0.33 μm/hr. RHEED patterns demonstrated a transition from the (2x2) Si surface to a (1x1) reconstruction as the film nucleated. Streaks broadened as growth progressed, indicating single-crystal material with some disorder. This disorder was further verified by X-ray double crystal rocking curves (DCRC) which showed either broad peaks (2700-6000 arc-sec) or no thin-film peak at all. The films were also examined by Auger Electron Spectroscopy (AES) and SIMS after growth, and indicated a slight sulfur deficiency. Growth kinetics, as described in the literature, indicate a slight Zn overpressure is needed. A single, solid source cannot provide this.

It is this demonstrated need to modulate constituent fluxes, as well as the ability to use H_2S gas to desorb the silica complex, which has provided the impetus to develop a "gas-source MBE" system. This system is presently being designed and uses a 2500 liter-sec (H_2) cryopump with a 220 liter-sec ion pump in the growth chamber. Sample manipulating, RHEED, AES, and a quadrupole mass spectrometer will also be available for in-situ analysis of the sample surface.

Theory of High Field Electronic Transport in Bulk ZnS and ZnSe

Kevin Brennan

School of Electrical Engineering

and

Microelectronics Research Center

Georgia Institute of Technology

Atlanta, Georgia 30332-0250

ABSTRACT

We present ensemble Monte Carlo calculations of electron transport in bulk ZnSe and ZnS under conditions of high applied electric field strengths. The calculations include the full details of the first two conduction bands as well as the full order treatment of the electron-phonon scattering mechanisms. The steady state electron drift velocities as a function of applied electric field are determined for each material system as well as the total electron-phonon scattering rates. In addition, the high field probability distribution function is presented for both ZnS and ZnSe. Interestingly, the electron distribution is much cooler in bulk ZnS than in bulk ZnSe at comparable electric field strengths even in the absence of significant impact ionization in either material. This implies that the threshold voltage for electroluminescent light emission will be correspondingly lower in comparable ZnSe devices than in ZnS structures. This result is in agreement with previous experimental observations of Shah et al. [Appl. Phys. Lett., 33, 995 (1978)].

Submitted to J. Applied Physics

1. Introduction

Thin-film electroluminescent devices have become of great interest since they offer a possible means of achieving a high resolution, light weight, compact video display panel for computer terminals or television screens [1,2]. Unfortunately, electroluminescent, EL, devices are at present highly inefficient, and can be made reliably to emit only in a few colors. Nevertheless, EL devices offer significant advantages over other existing technologies such as cathode ray tubes, plasma and liquid crystal displays [1].

High field electroluminescence was first reported in bulk ZnS [3] and has since been investigated in a host of new materials as an application of thin-film technology [4-11]. The basic mechanism of electroluminescence of use in thin film structures is based on high-field acceleration of majority carrier electrons to optical energies at which luminescent centers intentionally introduced into the host material can be impact excited. Either ac or dc power supplies can be used to provide the necessary carrier heating. The use of either power source provides different advantages in device performance.

The particular advantage of an ac EL device is that it suffers no performance deterioration as a function of time due to resistive effects. ac EL devices are essentially capacitive, since they are formed by encapsulating a large band-gap semiconductor, such as ZnSe:Mn or ZnS:Mn, by two insulating layers, typically Y_2O_3, on either side of the semiconductor. The ac bias applied across the device acts to alternately accelerate

the electrons from one semiconductor/insulator interface to the other. The source of charge carriers is at present believed to be the interface states formed at the semiconductor/insulator boundary [12,13]. Due to the relatively small number of interface states, the free carrier concentration is quite small < 1.0×10^{11} $1/cm^3$ [13] which limits the output brightness of the device.

dc EL devices, made using Schottky barriers, or metal-insulator-semiconductor layers are not limited by the number of free carriers available to impact excite the luminescent centers as are ac devices. The source of charge carriers is the metal electrode which provides virtually unlimited number of electrons. Nevertheless, performance deterioration with time, due to both electromigration of the luminescent centers and an increase in resistivity, is a critical disadvantage of dc EL displays.

The performance of any EL device, either ac or dc, depends upon the probability of an electron impact exciting a luminescent center which in turn depends upon the density of centers present in the semiconductor layer, the probability of an electron achieving the impact excitation threshold energy and the collision cross section itself. Present EL devices exhibit very poor overall efficiencies due to several reasons. First, the number of luminescent centers cannot be effectively increased much beyond 1-2% in concentration without causing quenching [12]. Secondly, the collision cross section, which is an inherent property of the center, cannot be readily engineered. Therefore, the efficiency can best be improved by increasing the number of hot electrons capable of impact exciting a center.

The most obvious means of heating the electron distribution to the energies necessary for impact excitation is through the application of an electric field. In general, this is a very inefficient process since the field heating is balanced, on average, by inelastic phonon scattering processes. The competing processes of field heating and phonon scatterings determines the average carrier energy and the shape of the overall nonequilibrium distribution function. Fluctuations from the average energy, arising from electrons gaining more energy from the field than is lost to the phonons, occur over small lengths of time. These carriers, which deviate from the average ensemble behavior, constitute the high energy tail of the distribution function and are responsible for both impact excitation and impact ionization events. Even at very high electric field strengths the number of carriers which survive to sufficiently high energies for impact excitation is limited.

The shape of the electron distribution function at high applied electric field strengths is difficult in general to determine. Previous theoretical investigations of electron transport in bulk ZnSe or ZnS [14,15] have been confined to determining the low field mobility as a function of temperature and impurity concentration. These investigations have done much to clarify the nature of electronic and hole transport [16] in bulk ZnSe but have not probed the physics of very high field transport in these materials at which electroluminescence occurs. In fact all of the previous models rely on an effective mass formulation as well as a first order treatment of the electron-phonon scattering rates. It is well known that both of these

approximations fail at high carrier energies. Therefore, a different approach must be used to study the nature of the high field carrier distribution functions.

In this paper we theoretically investigate the nature of electronic transport and the high energy tails of the electron distribution functions in bulk ZnSe and ZnS as a function of the applied electric field using a model particularly well tailored to very high field strengths. Our calculations are based on an ensemble, Monte Carlo model which includes the full details of the first two conduction bands derived from a pseudopotential band structure calculation [17,18]. The Monte Carlo calculation also includes a rigorous treatment of the electron-phonon scatterings based on a full order solution of the electron self-energy equation [19]. In this way, collisional broadening of the initial and final states is accounted for. Impact ionization is treated in both material systems based on the Keldysh model [20] assuming a soft ionization threshold [21,22]. The total electron-phonon scattering rates, calculated density of states and relevant material parameters used in the calculations are also presented.

2. Material Parameters and Electron-Phonon Scattering Rates

The material parameters used in the calculations of the electronic transport in bulk ZnSe and ZnS are collected in Tables I and II respectively. Little experimental work has been done to date on the fundamental parameters of each of these two material systems. Therefore, the parameters used in this analysis are not precisely known. Nevertheless, they represent the best known values presently available.

The gamma valley effective masses are based on experimental measurements [23] using cyclotron resonance techniques. Both the satellite valley effective masses and intervalley separation energies are difficult to determine experimentally and to the author's knowledge no such measurements exist. These parameters were determined directly from the empirical pseudopotential calculations of the band structures. Our band structure calculation for ZnSe is in good agreement with the work of Humphreys and Srivastava [17]. Their calculation is made using a nonlocal pseudopotential. On the basis of this approach it is found that the X valley lies lower in energy than the L valley with corresponding intervalley separation energies of 1.49 eV and 1.58 eV respectively. To the author's knowledge, no nonlocal pseudopotential calculations of the ZnS band structure exist. In the absence of such a calculation, we have used the empirical pseudopotential approach of Cohen and Bergstresser [18]. The X and L valleys are found to lie at roughly the same energy above the Γ valley minimum, $\sim$ 1.45 eV.

The sound velocities are determined from the measured phonon dispersion curves of Talwar et al. [24]. The optical phonon energies as well as the dielectric constants have also been selected from the literature [15,23].

The intervalley phonon energies and coupling constants are generally unknown even in the most studied semiconductors. At present no reliable means exists for determining the intervalley scattering parameters. Therefore, we have chosen identical sets for each material and have used similar values to those reported for GaAs and InP [25].

The importance of the intervalley parameters can be minimized by calculating the total scattering rate based on the numerically generated density of states. Our approach is as follows. We calculate the total scattering rate initially using the golden rule in both materials with the same choice of intervalley coupling constants and phonon energies as given in Tables I and II. The total scattering rate is then recalculated at roughly the onset of the intervalley deformation potential scattering using the full order solution of the electron self-energy equation. The integral equation is solved numerically including the exact density of states calculated from the pseudopotential method. The only adjustable parameter is then the overall coupling constant, g^2 [25], which is found from comparing the first order rate to the full order rate at low energy. In this way, the scattering rates are made less dependent upon the totally unknown intervalley deformation potentials and phonon energies. Instead the scattering rates are related to the better known final density of states.

The density of states of the first two conduction bands of ZnSe and ZnS, determined numerically from the pseudopotential calculations, are presented in Figures 1 and 2 respectively. It is interesting to note that the density of states exhibits two peaks widely separated in energy. The second peak in either figure is due to the presence of the second conduction band. In both materials, transport in the second conduction band is important since the carriers can attain very high energies prior to impact ionizing. In materials like GaAs and InP, the inclusion of the second conduction band is not as critical since the impact

ionization process acts to confine the carriers within the first conduction band by cutting off the very high energy tail. Few electrons survive to high enough energy to enter the second conduction band in GaAs or InP. In ZnSe or ZnS, the energy gap is greater than the width of the first conduction band. Therefore, the carriers must impact ionize from states within the second conduction band. Hence, its inclusion in high field calculations in which impact excitation and impact ionization events occur is crucial.

The total electron-phonon scattering rates, in the absence of impact ionization, as a function of carrier energy in ZnSe and ZnS are presented in Figures 3 and 4 respectively. It is important to note that the total scattering rate is greater in ZnS than in ZnSe throughout the range of interest here. This is due to two factors. The higher scattering rate in ZnS at low energies is due to the much larger electron effective mass and polar optical phonon energy. At higher energies, the scattering rate in ZnS is greater since the density of states is somewhat larger as seen in Figures 1 and 2. As we will see below, this greatly influences the electron drift velocities and carrier energies.

3. Steady-State Drift Velocities and Distribution Functions

The steady state electron drift velocities as a function of applied electric field in bulk ZnSe and ZnS are presented in Figures 5 and 6 respectively. The calculations are made at 300 K with the field oriented in the <100> crystallographic direction. From inspection of Figures 5 and 6 it is readily apparent that

the threshold field for intervalley transfer is much greater in ZnS than in ZnSe. This, at first, seems somewhat surprising since the intervalley threshold energies and intervalley scattering rates are essentially identical between the two materials. However, recent theoretical work [26] indicates that the threshold field depends predominately upon the strength of the polar optical phonon scattering and the electron effective mass within the gamma valley. The optical phonon energy and effective mass within the gamma valley are much greater in ZnS than in ZnSe which collectively act to confine the electrons within the central valley.

The effect of the optical phonon energy on the carrier temperature can be understood as follows. The phonon energy determines the amount of energy exchanged per collision between the electron and lattice subsystems. As the phonon energy increases more energy is transfered per collision. Owing to the much larger phonon emission than absorption rates, a greater phonon energy leads to more effective cooling of the electron distribution, and hence greater confinement in the gamma valley. The intervalley threshold field then is greater for materials in which the polar optical phonon energy is higher.

The much larger gamma valley effective mass in ZnS than in ZnSe also effects the intervalley threshold electric field. Clearly, the greater the effective mass the less energy the carrier gains per drift. Calculations in the AlGaAs and GaAs material systems [26] indicate that variations in the gamma valley mass influences the threshold field much more than the peak velocity. The results for ZnS and ZnSe reported here are in

accord with these conclusions.

The electron energy distribution functions at various electric field strengths are presented for ZnSe and ZnS in Figures 7 and 8 respectively. It is important to note that the electron distribution function is significantly cooler in ZnS than in ZnSe at comparable electric fields. Specifically, at 500 kV/cm, no carriers in ZnS survive to energies at which impact excitation processes can occur, ~ 2.3 eV. In fact, no electrons attain even 2.0 eV in energy. Conversely, in bulk ZnSe, a significant fraction of electrons, ~ 2-3 %, attain energies greater than or equal to 2.3 eV. Therefore, under comparable conditions ZnS electroluminescent devices should have a sizeably greater threshold voltage than ZnSe devices. This is in accord with experimental observations of thin film ZnSe:Mn and ZnS:Mn EL displays [5].

4. Conclusions

Based on ensemble Monte Carlo calculations of high field electronic transport in bulk ZnSe and ZnS it is found that the electron energy distribution function is significantly cooler in ZnS than in ZnSe at comparable electric field strengths. The cooler distribution in ZnS is due predominately to the much greater electron scattering rate, roughly twice as large as in ZnSe, within the gamma valley. Therefore, the electrons are more greatly confined within the gamma valley at comparable field strengths leading to an overall cooler distribution. This is clearly reflected as well by the greater threshold field in ZnS than in ZnSe. The larger gamma valley scattering rate in

ZnS is due to the much greater polar optical phonon energy and carrier effective mass.

In addition, the electron scattering rate is somewhat higher in ZnS than in ZnSe at energies above the intervalley threshold. Again, this acts to cool the carriers within the ZnS more than in the ZnSe.

Due to the much cooler electron distribution in ZnS, the threshold field for electroluminescence, which is a measure of the number of electrons at energies at which impact excitation processes can occur, is greater than in ZnSe. Consequently, EL displays made using ZnS will be less efficient than those employing ZnSe since a greater input power is necessary to achieve comparable output brightness. In either case, display efficiencies are poor due to the difficulty in heating significant carriers to the impact excitation threshold energy.

Alternatively, we have proposed a new approach, using a variably spaced superlattice [27,28], to efficiently heat electrons to high energies. The electrons sequentially tunnel through a multilayer stack under bias and emerge into an active semiconductor layer at an energy equal to the conduction band bending. The injection energy is chosen to correspond to the excitation energy of the luminescent centers within the active region [29]. In this way, the efficiency of the device is greatly enhanced since phonon cooling is defeated in heating the distribution.

Acknowledgements

The author would like to thank Dr. C. J. Summers for helpful discussions on this work. The technical assistance of D. Fouts and P. Knight at the Georgia Institute of Technology is gratefully appreciated. This work was sponsored by NASA under contract NAG 1-586.

REFERENCES

[1] T. S. Perry and P. Wallich, IEEE Spectrum, 22, 52 (1985).

[2] H. Kawarada and N. Ohshima, Proc. IEEE, 61, 907 (1973).

[3] G. Destriau, J. Chem. Phys., 33, 620 (1936).

[4] D. C. Morton and F. E. Williams, Appl. Phys. Lett., 35 671 (1979).

[5] J. Shah and A. E. DiGiovanni, Appl. Phys. Lett., 33, 995 (1978).

[6] F. J. Bryant, A. Krier, and G. Z. Zhong, Solid-State Electron., 28, 847 (1985).

[7] A. Vecht, N. J. Werring, R. Ellis, and P. J. F. Smith, Proc. IEEE, 61, 902 (1973).

[8] K. Okamoto and Y. Hamakawa, Appl. Phys. Lett., 35, 508 (1979).

[9] J. Benoit, P. Benalloul, R. Parrot, and J. Mattler, J. Lumin. 18/19, 739 (1979).

[10] V. Marrello, W. Ruehle, and A. Onton, Appl. Phys. Lett., 31, 452 (1977).

[11] H. Matsumoto, S. Tanaka, and T. Yabumoto, Jpn. J. Appl. Phys., 17, 1543 (1978).

[12] R. Mach and G. O. Muller, Phys. Status Solidi A, 69, 11 (1982).

[13] F. Williams, J. Lumin., 23, 1 (1981).

[14] M. Aven and B. Segall, Phys. Rev., 130, 81 (1963).

[15] H. E. Ruda, J. Appl. Phys., 59, 1220 (1986).

[16] H. E. Ruda, J. Appl. Phys., 59, 3516 (1986).

[17] T. P. Humphreys and G. P. Srivastava, Phys. Stat. Sol. B, 112 581 (1982).

[18] M. L. Cohen and T. K. Bergstresser, Phys. Rev., 141, 789 (1966).

[19] T. Wang, Ph.D. Thesis, Univ. of Ill., Urbana, 1986.

[20] L. V. Keldysh, Zh. Eksp. Teor. Fiz. 48, 1692 (1965) [Sov. Phys.-JETP, 21, 1135 (1965)]

[21] J. Y. Tang and K. Hess, IEEE Trans. Electron Dev., ED-29, 1906 (1982).

[22] R. C. Woods, Appl. Phys. Lett., 52, 65 (1988).

[23] B. Segall, in Physics and Chemistry of II-VI Compounds," edited by M. Aven and J. S. Prener (North-Holland, Amsterdam, 1967), 1-72.

[24] D. N. Talwar, M. Vandevyver, K. Kunc, and M. Zigone, Phys. Rev. B, 24, 741 (1981).

[25] K. Brennan and K. Hess, Solid State Electron., 27, 347 (1984).

[26] K. F. Brennan, D. H. Park, K. Hess, and M. A. Littlejohn, to be published, J. Appl. Phys.

[27] C. J. Summers and K. F. Brennan, Appl. Phys. Lett., 48, 806 (1986).

[28] C. J. Summers, K. F. Brennan, A. Torabi, and H. M. Harris, Appl. Phys. Lett., 52, 132 (1988).

[29] K. F. Brennan and C. J. Summers, J. Appl. Phys., 61, 5410 (1987).

Figure Captions

Figure 1: Density of states of the first two conduction bands of ZnSe in arbitrary units as a function of energy determined from the pseudopotential calculation of the band structure.

Figure 2: Density of states of the first two conduction bands of ZnS in arbitrary units as a function of energy determined from the pseudopotential calculation of the band structure.

Figure 3: Total electron-phonon scattering rate in bulk ZnSe as a function of energy at 300 K. Impact ionization is not included. The scattering rate is calculated using the full order electron self-energy equation along with the density of states presented in Figure 1.

Figure 4: Total electron-phonon scattering rate in bulk ZnS as a function of energy at 300 K. Impact ionization is not included. The scattering rate is calculated using the full order electron self-energy equation along with the density of states presented in Figure 2.

Figure 5: Steady-state electron drift velocity as a function of applied electric field in bulk ZnSe at 300 K. The field is applied in the <100> direction. The threshold field for intervalley transfer is found to be roughly 25 kV/cm.

Figure 6: Steady-state electron drift velocity as a function of applied electric field in bulk ZnS at 300 K. The threshold field for intervalley transfer is found to be

much greater than in bulk ZnSe, ~ 70 kV/cm owing to the greater confinement of the electrons in the gamma valley.

Figure 7: Electron energy distribution function calculated from the ensemble Monte Carlo simulation with the electric field as a parameter. The distribution function is divided by the density of states function giving the probability density as a function of energy. The distribution is sharply peaked at low energies due to the very small density of states there.

Figure 8: The electron energy distribution function calculated from the ensemble Monte Carlo simulation at various electric field strengths. The distribution is divided by the density of states function presented in Figure 2. Due to the very small density of states at low energies, the distribution is greatly peaked there.

Table I

ZnSe

Bulk Material Parameters

Parameter	Value
Lattice Constant (cm)	5.65×10^{-8}
Polar Optical Phonon Energy (eV)	0.031
Sound Velocity (cm/sec)	4.58×10^{5}
Low-Frequency Dielectric Constant	8.10
High-Frequency Dielectric Constant	5.90
Energy Band Gap (eV)	2.70
Impact Ionization Threshold Energy (eV)	3.20

Valley Dependent Parameters

Parameter	Γ	L	X
Effective Mass (m^*/m_o)	0.170	0.510	0.316
Nonparabolicity (eV^{-1})	0.690	0.650	0.360
Valley Separation (eV)	---	1.58	1.49
Optical Phonon Energy (eV)	---	0.031	0.031
Number of Equivalent Valley	1	4	3
Intervalley Deformation Potential (eV/cm)			
from Γ	0	1×10^{9}	1×10^{9}
from X	1×10^{9}	9×10^{8}	9×10^{8}
from L	1×10^{9}	1×10^{9}	9×10^{8}
Intervalley Phonon Energy			
from Γ	0.0	0.0267	0.0279
from X	0.0279	0.0273	0.0279
from L	0.0267	0.0267	0.0273

Table II

ZnS

Bulk Material Parameters

Parameter	Value
Lattice Constant (cm)	5.41×10^{-8}
Polar Optical Phonon Energy (eV)	0.044
Sound Velocity (cm/sec)	5.20×10^{5}
Low-Frequency Dielectric Constant	8.32
High-Frequency Dielectric Constant	5.13
Energy Band Gap (eV)	3.60
Impact Ionization Threshold Energy (eV)	3.60

Valley Dependent Parameters

Parameter	Γ	L	X
Effective Mass (m^*/m_o)	0.28	0.222	0.40
Nonparabolicity (eV^{-1})	0.690	0.650	0.360
Valley Separation (eV)	---	1.449	1.454
Optical Phonon Energy (eV)	---	0.044	0.044
Number of Equivalent Valley	1	4	3
Intervalley Deformation Potential (eV/cm)			
from Γ	0	1×10^{9}	1×10^{9}
from X	1×10^{9}	9×10^{8}	9×10^{8}
from L	1×10^{9}	1×10^{9}	9×10^{8}
Intervalley Phonon Energy			
from Γ	0.0	0.0267	0.0279
from X	0.0279	0.0273	0.0279
from L	0.0267	0.0267	0.0273

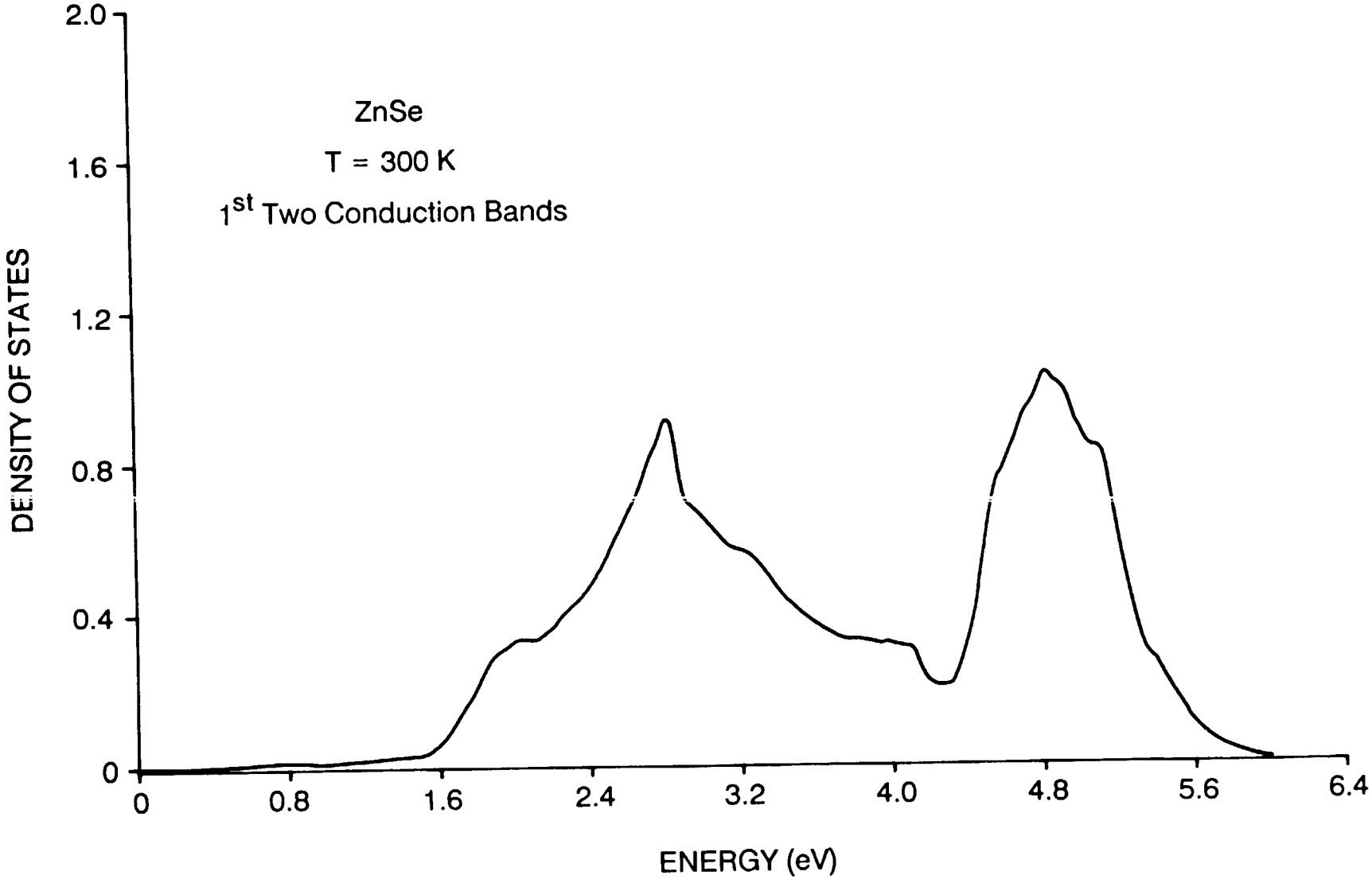

Figure 1
Brennan

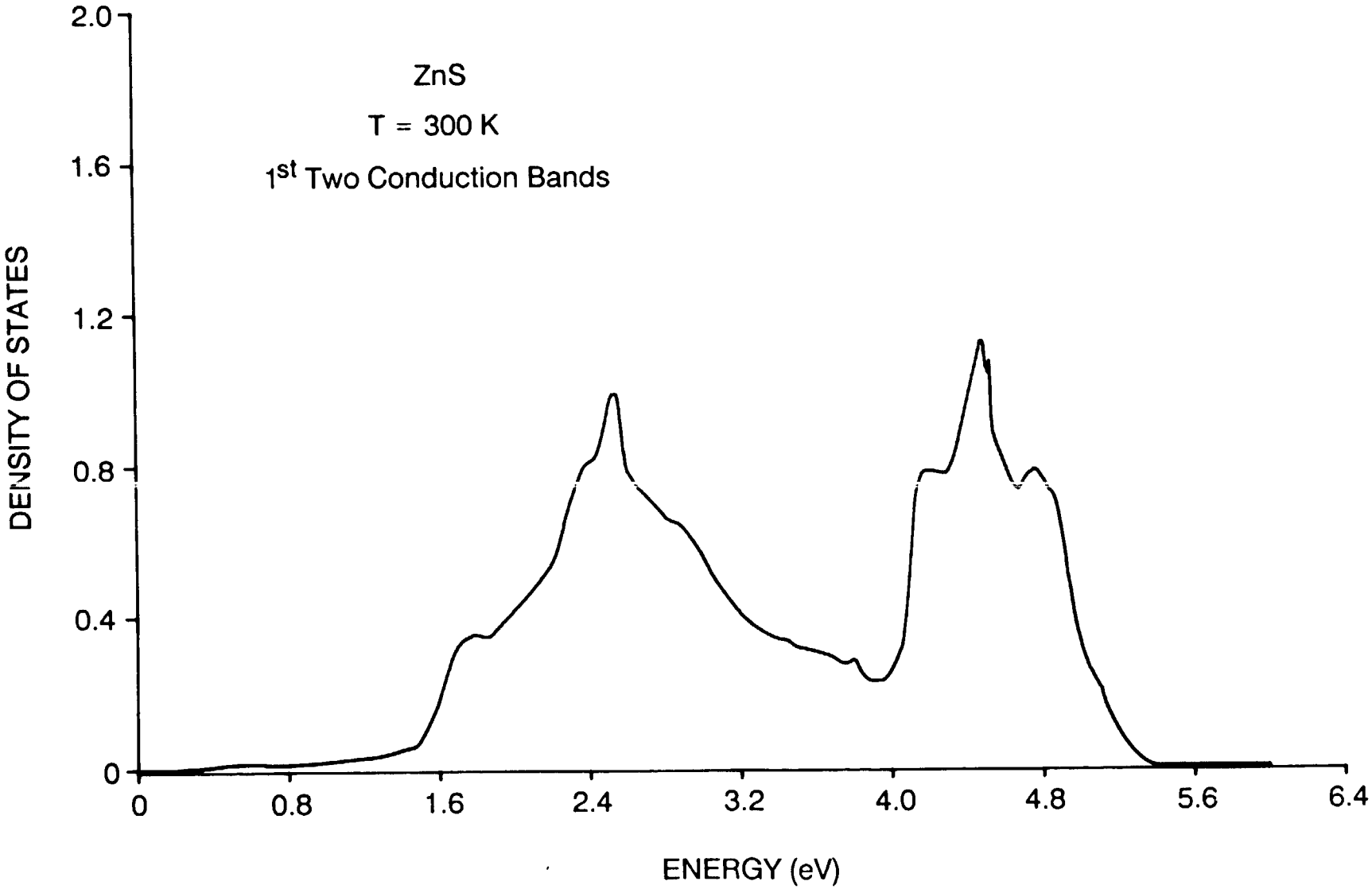

Figure 2
Brennan

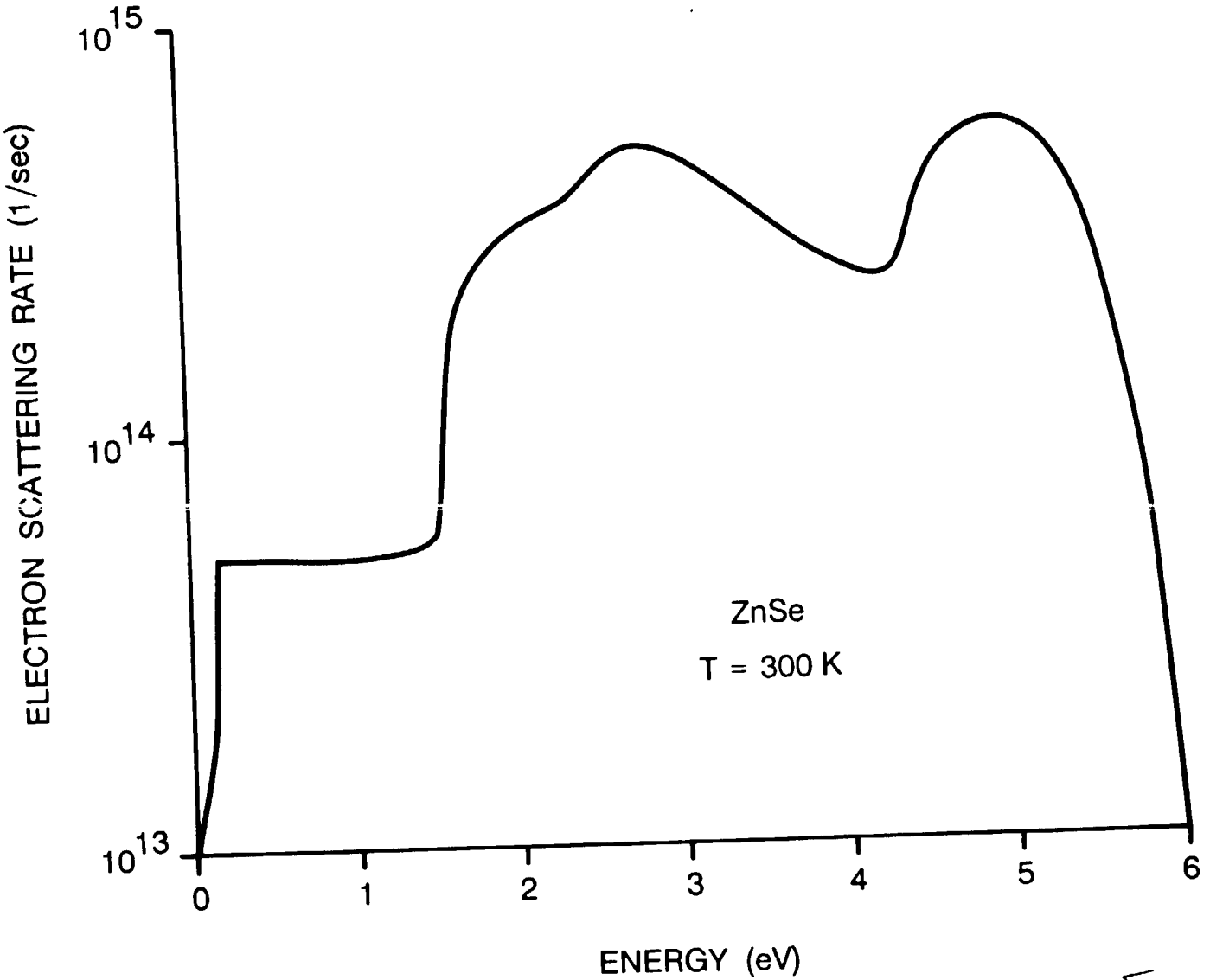

Figure 3
Brennan

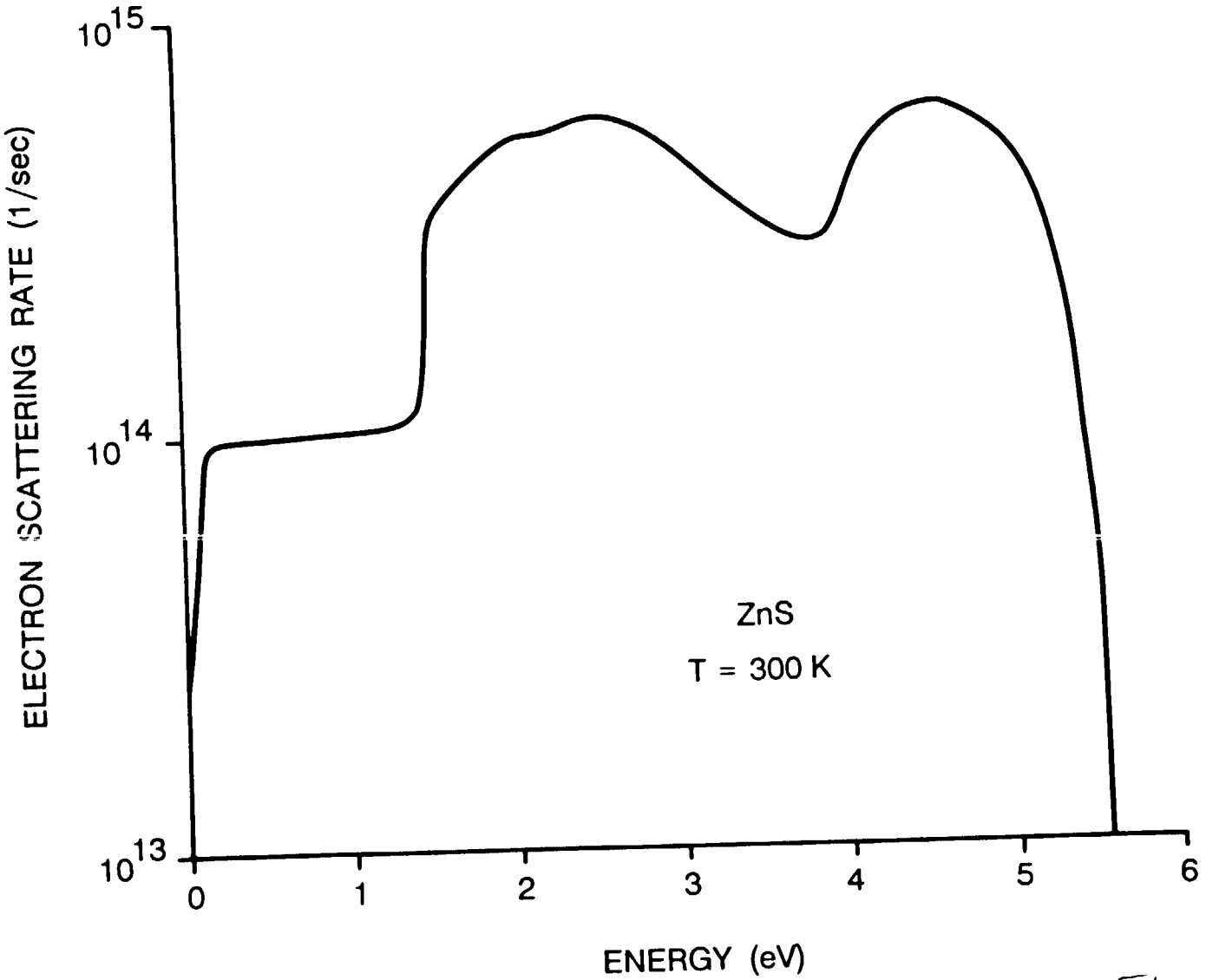

Figure 4
Brennan

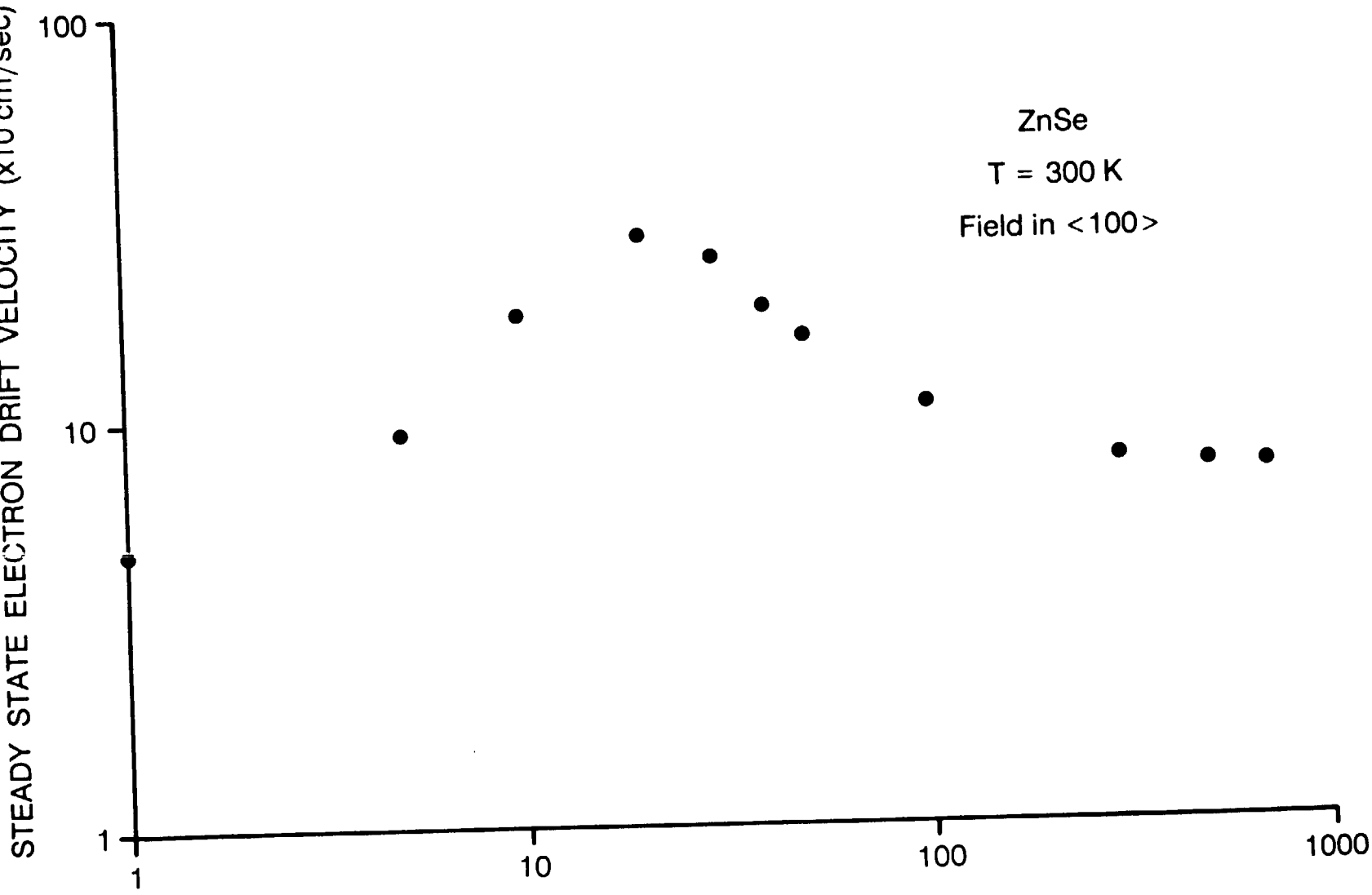

Figure 5
Brennan

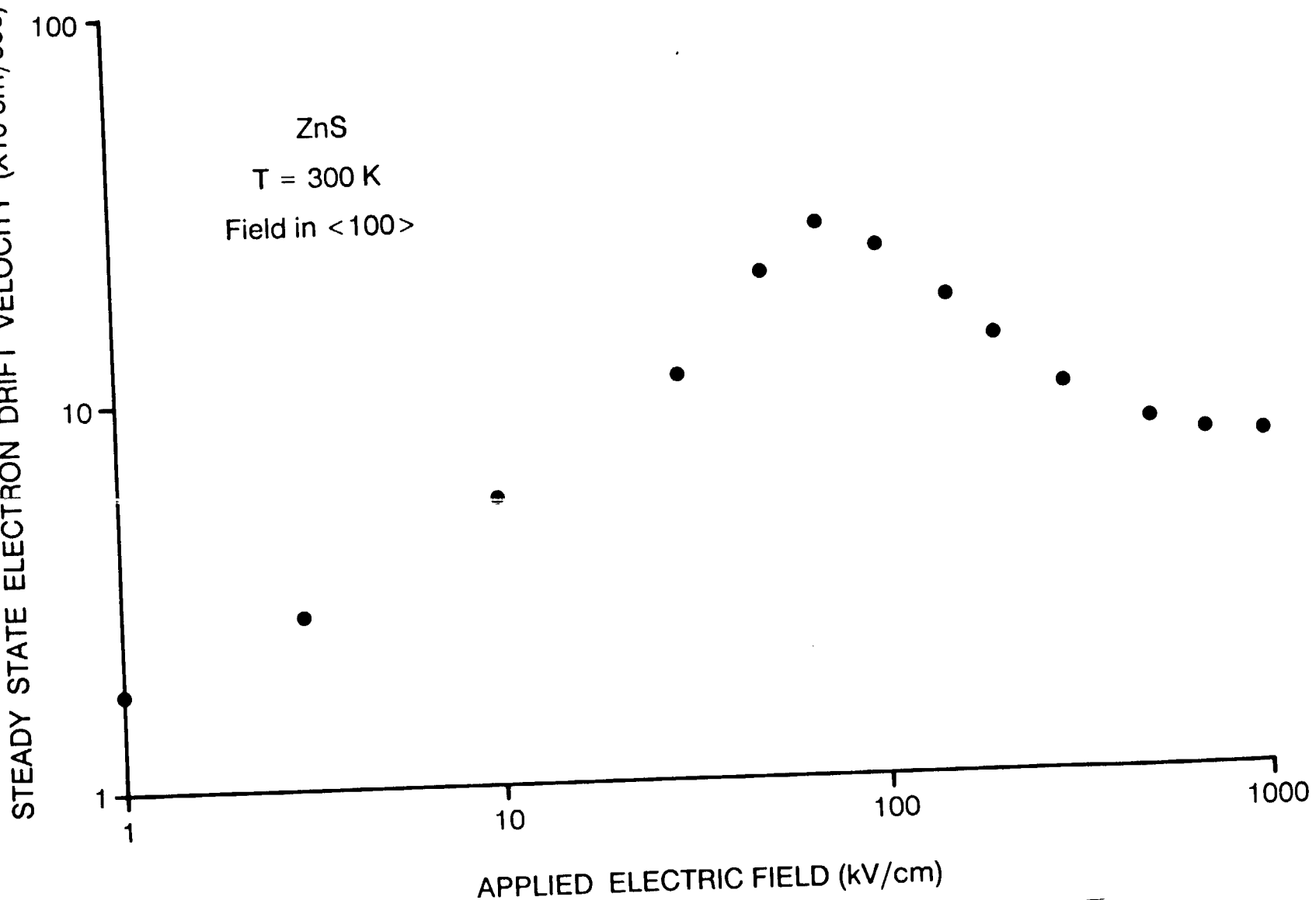

Figure 6
Brennan

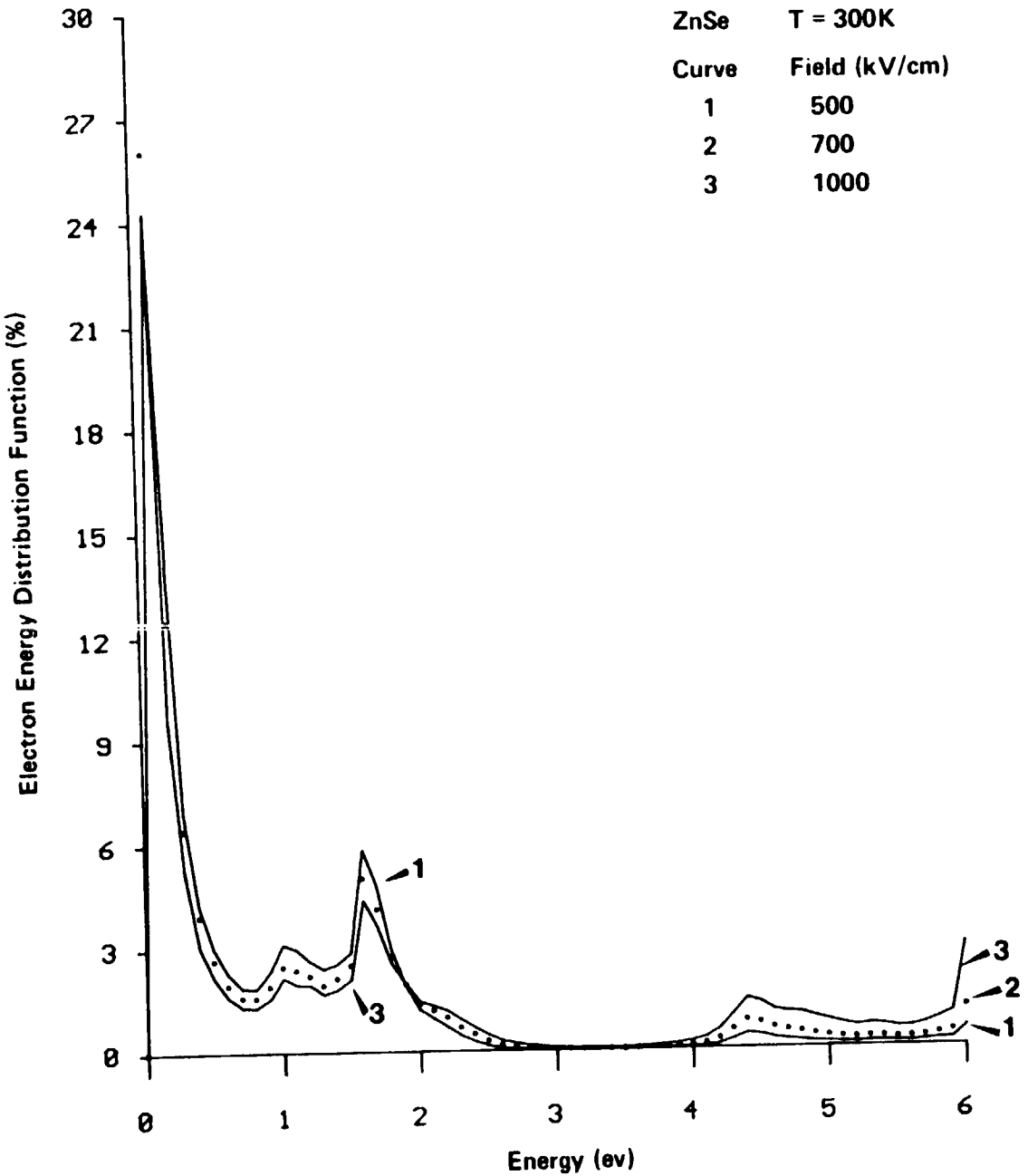

Fig 7
Brennan

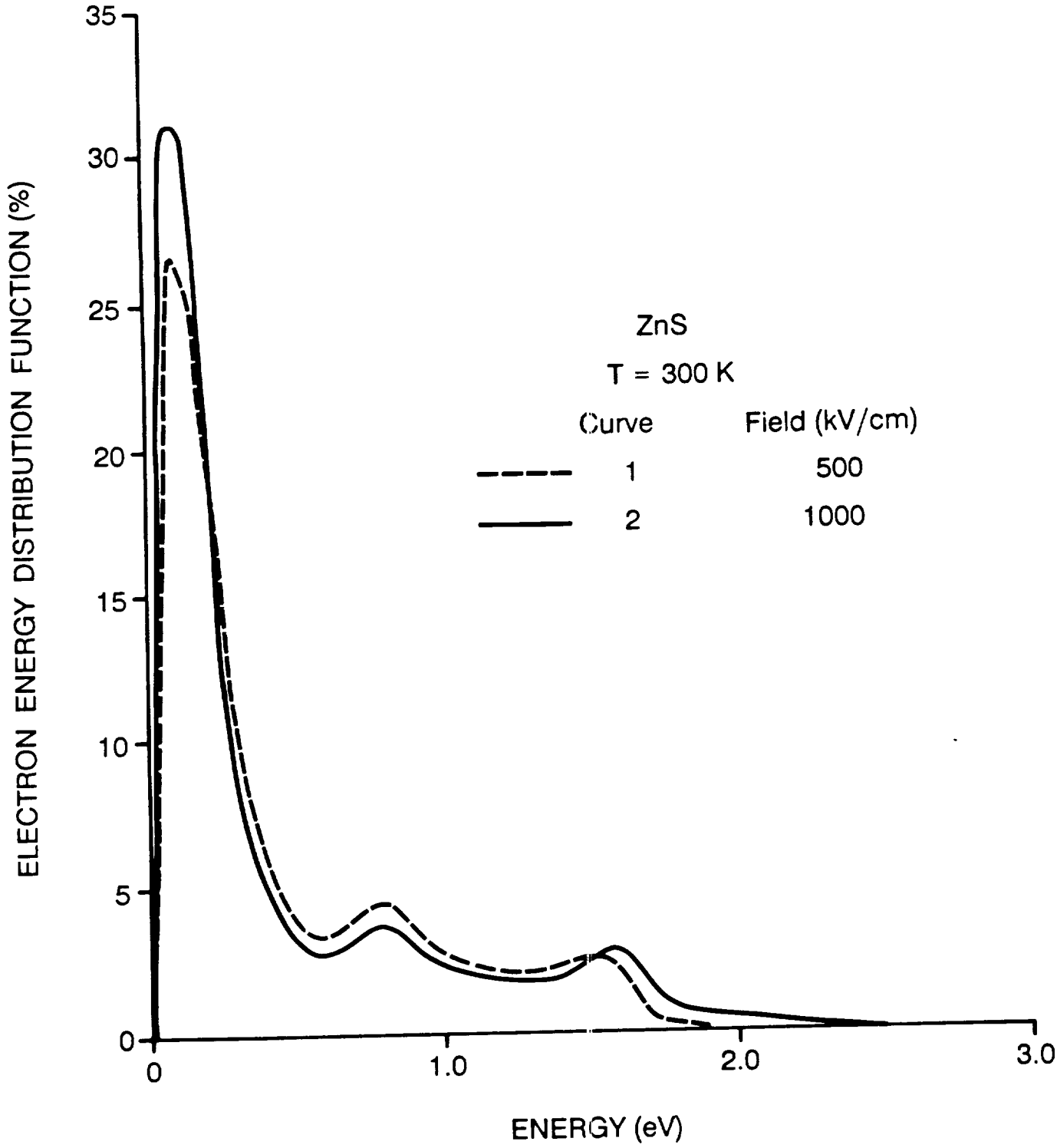

Fig 6
Brennan